Journal of Neuroscience Research 88:3498–3507 (2010)

Redox Proteomics in Aging Rat Brain: Involvement of Mitochondrial Reduced Glutathione Status and Mitochondrial Protein Oxidation in the Aging Process

M. Perluigi,[1] F. Di Domenico,[1] A. Giorgi,[1] M.E. Schininà,[1] R. Coccia,[1] C. Cini,[1] F. Bellia,[2] M.T. Cambria,[2] C. Cornelius,[2] D.A. Butterfield,[3] and V. Calabrese[2,4]*

[1]Department of Biochemical Sciences, "Sapienza" University of Rome, Rome, Italy
[2]Department of Chemical Sciences, University of Catania, Catania, Italy
[3]Department of Chemistry, Center of Membrane Science, and Sanders-Brown Center on Aging, University of Kentucky, Lexington, Kentucky
[4]National Institute of Biosystems and Biostructures, Catania Section, Catania, Italy

Increasing evidence supports the notion that increased oxidative stress is a fundamental cause in the aging process and in neurodegenerative diseases. As a result, a decline in cognitive function is generally associated with brain aging. Reactive oxygen species (ROS) are highly reactive intermediates, which can modify proteins, nucleic acids, and polyunsaturated fatty acids, leading to neuronal damage. Because proteins are major components of biological systems and play key roles in a variety of cellular functions, oxidative damage to proteins represents a primary event observed in aging and age-related neurodegenerative disorders. In the present study, with a redox proteomics approach, we identified mitochondrial oxidatively modified proteins as a function of brain aging, specifically in those brain regions, such as cortex and hippocampus, that are commonly affected by the aging process. In all brain regions examined, many of the identified proteins were energy-related, such as pyruvate kinase, ATP synthase, aldolase, creatine kinase, and α-enolase. These alterations were associated with significant changes in both cytosolic and mitochondrial redox status in all brain regions analyzed. Our finding is in line with current literature postulating that free radical damage and decreased energy production are characteristic hallmarks of the aging process. In additon, our results further contribute to identifying common pathological pathways involved both in aging and in neurodegenerative disease development.

Key words: aging; proteomics; central nervous system; neurodegeneration; oxidative stress

Aging is a complex biological process characterized by a gradual decline in biochemical and physiological functions of most organs and is considered one of the most significant risk factors for age-related neurodegenerative diseases, such as Alzheimer's disease (AD), Parkinson's disease (PD), amyotrophic lateral sclerosis (ALS), Huntington disease, Fredreich ataxia, and multiple sclerosis (Mattson 2004; Calabrese et al., 2009a, 2010a,b). Age-related changes in the brain include reduction of trophic supports, decreased proteosomal enzyme activities, mitochondrial dysfunction, and change in the redox status, which promotes a more proinflammatory environment associated with increased formation of reactive oxygen species (ROS; Ashok and Ali, 1999; Zhu et al., 2006). The free radical theory of aging postulates that ROS may produce oxidative damage directly to critical biological molecules, including proteins, DNA, and lipids (Harman, 1992; Butterfield et al., 1998; Zhu et al., 2006).

In particular, the aging process is accompanied by a general decline in physiological functions in the CNS, which is particularly vulnerable to oxidative injury for its high oxygen consumption per unit weight, consistent with the generation of high levels of ROS, and the small amount of ROS defense systems (lower in the nervous system than in other tissues). Because the brain contains high levels of polyunsaturated fatty acids, which upon oxidation form neurotoxic lipid peroxidation products (MDA, HNE), neuronal tissue is extremely vulnerable to oxidative modification of its cellular components. The oxidative damage to cellular macromolecules accumulates with age and has been postulated to be the main, but

M. Perluigi and F. Di Domenico contributed equally to this work.

Contract grant sponsor: MIUR; Contract grant sponsor: FIRB; Contract grant number: RBRN07BMCT; Contract grant sponsor: INBB; Contract grant sponsor: "Fondi Ateneo."

*Correspondence to: Vittorio Calabrese, University of Catania—Chemistry, viale Andrea Doria 6, Catania 95125, Italy. E-mail: calabres@unict.it

Received 20 February 2010; Revised 11 July 2010; Accepted 16 July 2010

Published online 8 October 2010 in Wiley Online Library (wileyonlinelibrary.com). DOI: 10.1002/jnr.22500

not the only, type of endogenous damage strongly involved in the aging process (Beckman and Ames, 1998). Indeed, when postmitotic neurons are injured by oxidative stress, they cannot be replaced, carrying the detrimental effects of oxidative injury over the lifetime of the neuron population. The chemical reactions resulting from attacks of ROS/RNS on proteins are complex and lead to a variety of products, many as yet uncharacterized. The oxidative damage to proteins is reflected by increasing levels of protein carbonyls and decreasing levels of protein thiols (Stadtman, 1988; Stadtman and Berlett, 1998). Protein carbonylation, among different types of posttranslational modifications, serves as useful biomarker for the accumulation of oxidatively modified proteins (Stadtman, 1988). It appears that such modifications target very specific proteins and can affect the integrity and functioning of the proteome.

Several studies have indicated that the levels of oxidized proteins, exhibiting carbonyl groups, increase progressively with age in brain extracts of rats of different ages (Carney et al., 1991). Furthermore, because of their central role in producing energy (ATP), mitochondria were brought to attention in aging biology, in order to understand the decline of basal metabolic rate and, consequently, physiological performance observed in aged mammals. Mitochondria produce the majority of free radicals, and as a powerful source of these toxic oxidants are also their potential victim (Calabrese et al., 2001). In fact, the mitochondrial components (e.g., mtDNA or mt enzymes) are surely more susceptible to oxidative damage than all the other components (Lenaz et al., 2002; Boveris and Navarro, 2008). This damage increase might have important consequences for mitochondrial structure, for the activity of the respiratory chain complex, and for the global functionality of these organelles. An increasing body of evidence also suggests that the decay of mitochondria accompanied by an impairment of cell energy metabolism is an important factor in the pathogenesis of most important neurodegenerative disorders (Van Remmen and Richardson, 2001).

In this study, we examine the free radical hypothesis of aging, employing a redox proteomics technique. We conducted parallel analyses on both the oxidation of specific proteins, as assessed by elevated protein carbonyl levels, and the cellular redox state of cytosolic and mitochondrial glutathione in different brain regions of senescent (28 months) vs. aged (12 months) control rats. The results of this study show several proteins that are specifically oxidized by aging in the different brain regions examined, most of them being related to mitochondrial function and energy metabolism but also endowed chaperon activities. In addition, comparative analysis among patterns of protein oxidation revealed some common traits. The implications and the possible significance of oxidative modifications of these proteins together with their implications for the possible molecular targets and mechanisms associated with age-related decline of cellular function are discussed.

TABLE I. Percentage Energy Composition of AIN Diet (g/100 g)

Dextrin-Maltose[a]	53
Oil mixture[b]	25
Casein	22
D-L methionine	0.5
Salt mixture (AIN 76)	3.5
Vitamin mixture (AIN 76)	1.2

[a]From corn starch.
[b]Olive oil/corn oil 2:1; 16:0 = 12.8%; 16:1 = 0.4%; 18:0 = 5.2%; 18:1 = 27.8%; 18:2 = 50.4%.

MATERIALS AND METHODS

Chemicals

5,5′-Dithiobis-(2-nitrobenzoic acid; DTNB), 1,1,3,3-tetraethoxypropane, purified bovine blood SOD, NADH, reduced glutathione (GSH), oxidized glutathione (GSSG), β-NADPH (type 1, tetrasodium salt), glutathione reductase (GR; type II from bakers yeast), SIN-1 (3-morpholinosydnonimine hydrochloridte) were from Sigma (St. Louis, MO). All other chemicals were from Merck (Darmstadt, Germany) and of the highest grade available.

Animals and Samples Preparation

All animal protocols were approved by the University of Catania Laboratory Animal Care Advisory Committee. Male Wistar rats purchased from Harlan (Udine, Italy) were maintained in a temperature- and humidity-controlled room with a 12-hr light:dark cycle. Rats (n = 8, per group) of 12 (aged) and 28 (senescent) months were fed ad libitum a certified diet prepared according to the recommendations of the AIN, and the percentage energy composition is given in Table I. After sacrifice, brains were quickly removed and dissected into hippocampus, cortex, striatum, and cerebellum according to a standardized procedure, in a cold anatomical chamber and following a protocol that allows a maximum of 50 sec time variability for each sample across animals. Brain samples were minced and suspended in 10 mM HEPES buffer (pH 7.4) containing 137 mM NaCl, 4.6 mM KCl, 1.1 mM KH_2PO_4, 0.1 mM EDTA, and 0.6 mM $MgSO_4$ as well as proteinase inhibitors: leupeptin (0.5 mg/ml), pepstatin (0.7 μg/ml), type II S soybean trypsin inhibitor (0.5 μg/ml), and PMSF (40 μg/ml). Homogenates were centrifuged at 14,000*g* for 10 min to remove debris. Protein concentration in the supernatant was determined by the ''Coomassie Plus Protein Assay'' (Pierce, Rockford, IL).

Two-Dimensional Gel Electrophoresis

Samples (200 μg) were incubated at room temperature for 30 min in four volumes of 10 mM 2,4-dinitrophenylhydrazine (DNPH) in either 2 M HCl for protein carbonyl derivatization/oxyblots or 2 M HCl for gel maps and mass spectrometry analysis. This was followed by precipitation of proteins by addition of ice-cold 100% trichloroacetic acid (TCA) to a final concentration of 15%, and samples were placed on ice for 10 min. After centrifugation and washing with ethanol/ethyl acetate solution three times, the samples were then dissolved with 185 μl of

rehydration buffer (8 M urea, 20 mM dithiothreitol, 2.0% (w/v) CHAPS, 0.2% biolytes, 2 M thiourea, and bromophenol blue). For the first-dimension electrophoresis, 200 μl of sample solution was applied to IPG Strips, pH 3–10 (Bio-Rad, Hercules, CA). The isoelectric focusing was performed at 300 V for 2 hr linearly; 500 V for 2 hr linearly; 1,000 V for 2 hr linearly, 8,000 V for 8 hr linearly, and 8,000 V for 10 hr rapidly. All the processes described above were carried out at 22°C. The focused IEF strip was stored at –80°C until second-dimension electrophoresis was performed. For second-dimension electrophoresis, thawed strips were equilibrated for 10 min in 50 mM Tris-HCl (pH 6.8) containing 6 M urea, 1% (w/v) sodium dodecyl sulfate (SDS), 30% (v/v) glycerol, and 0.5% dithiothreitol and then reequilibrated for 15 min in the same buffer containing 4.5% iodacetamide in place of dithiothreitol. Linear gradient (8–16%) precast criterion Tris-HCl gels (Bio-Rad) were used to perform second-dimension electrophoresis. After electrophoresis, the gels were incubated in fixing solution (7% acetic acid, 10% methanol) for 20 min. Approximately 40 ml of Coomassie Safe Gel Stain (Bio-Rad) was used to stain the gels for 1 hr, on a gently continuous rocker. The gels were placed in deionized water overnight for destaining.

Western Blotting

The same amount of protein samples (200 μg) was used for detecting specific protein carbonyl levels, and the electrophoresis was carried out in the same way as described above. Proteins (200 μg) were incubated with 4 volumes of 20 mM 2,4-dinitrophenylhydrazine (DNPH) at room temperature (25°C) for 20 min. The gels were prepared in the same manner as for 2D electrophoresis. The proteins from the second-dimension electrophoresis gels were transferred to nitrocellulose (Bio-Rad) using a Criterion Blotter Apparatus (Bio-Rad) at 15 V for 2 hr. The 2,4-dinitrophenyl hydrazone (DNP) adducts of the carbonyls of the proteins were detected on the nitrocellulose paper using a primary rabbit antibody (Chemicon, Temecula, CA) specific for DNP protein adduct (1:100), followed by a secondary goat anti-rabbit IgG (Sigma, St. Louis, MO) alkaline-phopsphatase conjugated antibody. The resulting stain was developed using 5-bromo-4-chloro-3-indolyl phosphate/nitro blue tetrazolium (BCIP/NBT) solution (SigmaFast tablets; Sigma).

Image Analysis

The gels (n = 8 aged and n = 8 senescent) and nitrocellulose blots were scanned with a GS-800 Densitometer (Bio-Rad). PDQuest 2-D Analysis Software (Bio-Rad, Inc.) was used for matching and analysis of visualized protein spots among differential gels and membranes to compare protein and DNP immunoreactivity content between senescent and aged rats brain samples. This sophisticated software offers powerful comparative analysis and is specifically designed to analyze many gels or blots at once. Powerful automatching algorithms quickly and accurately match gels or blots, and sophisticated statistical analysis tools identify experimentally significant spots. After completion of spot matching, the normalized intensity of each protein spot from individual gels (or membranes) was compared between groups using statistical analysis. Statistical significance was assessed by a two-tailed Student's *t*-test. $P < 0.05$ was considered significant for comparison between aged and senescent rats.

Protein Identification by Mass Spectrometry

Selected spots were manually excised from gels and subjected to trypsin proteolysis. Briefly, after three destaining steps using a solution of 50 mM ammonium bicarbonate (5 min), 50% acetonitrile in 50 mM ammonium bicarbonate (15 min), and 100% acetonitrile (15 min), about 100 ng trypsin (Trypsin Gold, Mass Spectrometry Grade; Promega, Madison, WI), solubilized in 10 μl of a 25 mM ammonium bicarbonate digestion buffer, was added to each vacuum-dried gel spot. Digestion was performed at 37°C overnight. An aliquot (1 μl) of each peptide mixture was mixed with the same volume of α-cyano-4-hydroxy-trans-cinnamic acid matrix solution (10 mg/ml) in 70% acetonitrile containing 0.2% TFA (v/v) and spotted onto a MALDI target plate. MALDI-ToF MS analyses were performed in a Voyager-DE STR instrument (Applied Biosystems, Framingham, MA) equipped with a 337-nm nitrogen laser and operating in reflector mode. Mass data were obtained by accumulating several spectra from laser shots with an accelerating voltage of 20 kV. Two tryptic autolytic peptides were used for the internal calibration (m/z 842.5100 and 2,807.3145). Identification by peptide mass fingerprint (PMF), with the monoisotopic mass list obtained from each spot, was performed after exclusion of expected contaminant mass values by the Peak Erazor program (http://www.protein.sdu.dk/gpmaw/Help/PeakErazor/peakerazor.html), using the Mascot search engine (v. 2.2) against the SwissProt database (v. 55.3, 36,6226 sequences). Up to one missed cleavage, 50 ppm measurement tolerance, oxidation at methionine (variable modification), and carbamidomethyl cysteine (fixed modification) were considered. Posttraslational modifications were not considered. Identifications were validated when the probability-based Mowse protein score was significant according to Mascot.

Determination of Glutathione and Glutathione Disulfide in the Cytosol

Brain regions were homogenized on ice for 10 sec in 100 mM potassium phosphate, pH 7.5, which contained 12 mM disodium EDTA. The homogenate was divided into two aliquot. For total glutathione (GSH + GSSG) assay, 0.25 ml of homogenate was added to an equal volume of 100 mM potassium phosphate buffer pH7.5, containing 17.5 mM EDTA and 10 mM 5,5′-dithiobis-(2-nitrobenzoic acid; DTNB; sample SS1). For oxidized glutathione (GSSG) assay, 0.25 ml of homogenate was added to 100 mM potassium phosphate buffer, pH 6.5, containing 17.5 mM EDTA and 10 mM N-ethylmaleimide NEM (sample SS2). The samples were centrifuged at 800*g* for 20 min, and the supernatant fractions were then centrifuged at 10,000*g* for 30 min. The supernatants of SS1 and SS2 represented the cytosolic fractions and were used for the spectrophotometrc assay of total or oxidized glutathione. Before spectrophotometric determination, a 0.25-ml aliquot of SS2 sample was passed through a C18 Sep-Pak

cartridge (Waters, Watford, United Kingdom) to remove the excess of NEM and washed with 0.5 ml of buffer, 100 mM potassium phosphate buffer, pH 7.5, containing 5 mM EDTA. Spectrophotometric assay of glutathione was performed adding the samples to a cuvette containing 0.5 units glutathione reductase, 0.2 mM DTNB in a final volume of 1 ml of 100 mM potassium phosphate buffer, pH 7.5, 5 mM EDTA, and the reaction initiated by adding NADPH (220 nmoles). The change in absorbance at 412 nm was recorded over a period of 5 min for SS1 sample or 10 min for SS2 sample using a reference cuvette containing equal concentrations of NADPH, DTNB, and enzyme. The GSH and GSSG content, expressed as nmol/mg protein, was determined by comparison with a standard curve obtained with GSH and GSSG solution.

Determination of Total Glutathione (GSH + GSSG) and Glutathione Disulfide (GSSG) in Mitochondria

The pellet of SS1 and SS2 samples obtained after centrifugation at 10,000*g* was utilized for determination of total and oxidized glutathione in mitochondria. The SS1 pellet was resuspended in 0.32 M sucrose, 1 mM EDTA, 10 mM Tris, pH 7.4, 5 mM DTNB. The SS2 pellet was resuspended in 0.32 M sucrose, 1 mM EDTA, 100 mM potassium phosphate buffer, pH 6.5, containing 5mM N-ethylmaleimide (NEM). Low- and high-speed differential centrifugations for mitochondrial isolation were, respectively, 1,300*g* for 3 min and 21,200*g* for 10 min for all brain regions examined; mitochondrial preparations were washed once with 100 mM potassium phosphate buffer, pH 7.5, containing 5 mM EDTA. This washing step was found to be critical to remove excess GSH and GSSG from the cytosolic fraction. The mitochondria were then mixed, sonicated, and centrifuged at 10,000*g* for 11 min, the supernatant was used for spectrophotometric determination assay as described above.

Enzyme Assays

Pyruvate kinase. The enzyme activity of pyruvate kinase (PK) was determined at 37°C by lactate dehydrogenase-coupled spectrophotometric assay. The standard reaction mixture contained 100 mM Tris, pH 8.0, 100 mM KCl, 10 mM $MgCl_2$, 0.5 mM EDTA, 0.2 mM NADH, 10 μg LDH, 10 mM phosphoenolpyruvate, and 1.5 mM ADP in a final volume of 1 ml. One unit of activity is the amount of enzyme catalyzing the oxidation of 1 μmol NADH/min under these conditions. The assay was carried out in a microplate reader (Labsystem Multiscan MS).

Glyceraldehyde-3-phosphate dehydrogenase. To determine the activity of GAPDH, 20 μg protein homogenate was added to an assay mixture (100 mM 3-phosphoglyceric acid, 200 U/ml 3-phosphoglyceric phosphokinase, 200 mM cysteine, 100 mM $MgSO_4$, 34 mM ATP, 7.0 mM β-NADH) in a UV-transparent microtiter plate (Corning). The change in absorbance at 340 nm was monitored during a 5-min period with a microplate reader (Labsystem Multiscan MS).

Statistical Analysis

Results are expressed as mean ± SEM of at least eight separate experiments. Statistical analyses were performed in the software package Systat (Systat, Evanston, IL). The significance of the differences, evaluated by two-way ANOVA, followed by Duncan's new multiple-range test, was considered significant at $P < 0.05$. The significance of the change in carbonylation of specific proteins in the proteomics study was evaluated via nonparametric Mann-Whitney-Wilcoxon test. $P < 0.05$ was considered statistically significant. As discussed extensively by Maurer et al. (2005), the proteome set of excessively carbonylated proteins with only several protein spots is much smaller than the microarray data sets with at least several thousand genes. Consequently, with this low number of proteins, microarray algorithms and statistical approaches are not applicable for proteomics, so we relied on the nonparametric Mann-Whitney-Wilcoxon for the small sample size.

RESULTS

Western blot and subsequent immunochemical detection of DNP adducts allowed identification of carbonylated proteins in the cerebral tissue samples of senescent in comparison with aged rats. We used a parallel approach to quantify the protein levels by Coomassie staining and the carbonyl levels by immunohistochemistry. Coomassie stain achieves a linear and sensitive staining of gel slabs, and immunoblotting with DNP antibody allows specific detection of DNP adducts in hippocampus samples. The specific carbonyl levels were obtained by dividing the carbonyl level of a protein spot on the nitrocellulose membrane by the protein level of its corresponding protein spot on the gel. Such numbers give the carbonyl level per unit of protein. Figure 1 shows representative 2D-electrophoresis gels of hippocampus from senescent (Fig. 1B) and aged (Fig. 1A) rats after Coomassie staining. Figure 2 shows representative 2D Western blots of senescent (Fig. 2B) and aged (Fig. 2A) rats. Compared with aged rats, senescent animals showed significantly higher levels of oxidation, and the identified proteins were: heat shock protein 90 (Hsp90), cytochrome b-c1 complex subnit 1, creatine kinase, malate dehydrogenase, α-enolase, glutamate dehydrogenase, pyruvate kinase, fructose-bishosphate aldolase C, ATP synthase subnit alpha, and glutamine synthase. Table II shows these proteins as identified by mass spectrometry along with the peptides matched, percentage coverage, pI, Mw values, and increase of specific carbonyl levels, indexed as percetange of control. In senescent rat cortex, creatine kinase B-type, serine/threonine-protein phosphatase 2B catalytic subunit alpha isoforms, aspartate aminotransferase, fructose-bisphosphate aldolase A, peroxiredoxin-2, guanine nucleotide-binding protein subunit beta-1, vacuolar ATP synthase subunit B, Hsp-70 heat shock protein, aldehyde dehydrogenase, pyruvate kinase isozymes M1/M2, ATP synthase subunit alpha, and triosephosphate isomerase were found with significantly higher levels of oxidation than controls (Table III). In senescent rat striatum, 78-kDa glucose-regulated

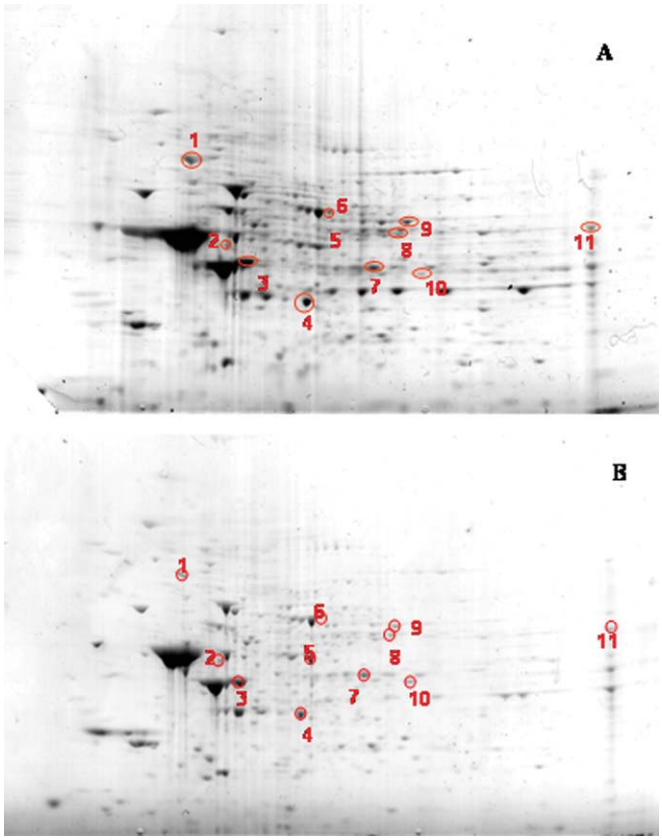

Fig. 1. Representative 2-D gels of aged (**A**) and senescent (**B**) rat hippocampus. Proteins (150 μg) were separated on immobilized pH 3–10 IPG strips followed by separation on 8–16% gradient SDS-PAGE gels and stained with Biosafe Coomassie. [Color figure can be viewed in the online issue, which is available at wileyonlinelibrary.com.]

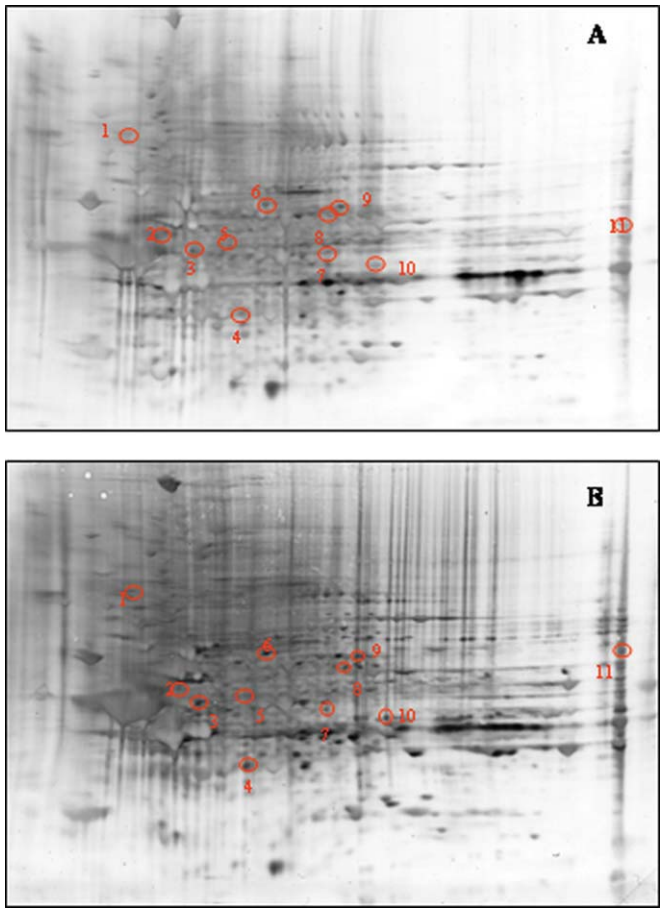

Fig. 2. Two-dimensional carbonyl immunoblots from aged (**A**) and senescent (**B**) rat hippocampus. Relative change in carbonyl immunoreactivity, after normalization of the immunostaining intensities to the protein content, was significant for six proteins. See text. [Color figure can be viewed in the online issue, which is available at wileyonlinelibrary.com.]

protein, Hsp-70 heat shock protein, adenylate kinase, elongation factor Tu, pyruvate kinase isozymes M1/M2, aconitate hydratase, triosephosphate isomerase, and glyceraldehyde-3-phosphate dehydrogenase showed higher levels of oxidation than in controls (Table IV).

All the proteins identified, except for pyruvate kinase isozymes M1/M2, occur in a single spot, being identified as a single spot on the gel, and present a significant P value (<0.05). Table V reports the proteins found to be significantly more oxidized in senescent rats cerebellum than in aged controls. These are heat shock cognate (Hsc) 70 protein, malate dehydrogenase, isocitrate dehydrogenase, vesicle-fusing ATPase, pyruvate kinase isozymes M1/M2, aspartate aminotransferase, phosphoglycerate kinase 1, voltage-dependent anion-selective channel protein, and adenylate kinase isoenzyme 4.

To verify the results obtained through redox proteomics analysis, we performed a validation study on the Hsp70 carbonylation using traditional immunochemistry. Consistently with the proteomics results, the carbonyl levels of Hsp70 were significantly increased by about 40% in cerebral cortex of senescent rats compared with aged rats (Fig. 3).

The contents of GSH and GSSG were measured in both cytosol and mitochondria of different brain regions of aged and senescent rats. In senescente rats, GSH was significantly ($P < 0.05$) diminished in all brain regions examined except for the cerebellum, where this decrease was not significant, compared with aged control animals (Fig. 4A). Consistently with this finding, mitochondrial GSH showed a significant decrease in all regions, particularly in the brain areas of hippocampus, followed by cortex, striatum, and cerebellum (Fig. 4A). Analysis of GSSG in the same brain regions showed significantly increases in senescent rat brain areas, both in the cytosol and in the mitochondrial compartments, particularly in the hippocampus, followed by striatum, cortex, and cerebellum (Fig. 4B). We also measured GSH/GSSH ratios in the different brain regions examined. In the cytosol, GSH/GSSG ratios varied in the brain from 87.2 ± 11 of aged to 33.5 ± 8 of senescent animals, whereas mitochondrial ratios of GSH/GSSG varied from 56.3 ± 9 to 19.9 ± 7, that is, 62% and 64%, respectively, indicating

TABLE II. Summary of the Proteins Identified by Redox Proteomics that are Increasingly Carbonylated in the Hippocampus from Senescent Rats vs Aged Rats[†]

Spot no.[†]	Protein name	*P* value	Fold oxidation	MOWSE score★	Mr/pI
1	Heat shock protein HSP 90-beta	<0.05	5.3	169	83571/4.97
2	Cytochrome b-c1 complex subunit 1, mitochondrial precursor	<0.01	10.8	139	53500/5.57
3	Creatine kinase B-type	<0.05	5	181	42983/5.39
4	Malate dehydrogenase cytoplasmic	<0.04	9.4	144	36631/6.16
5	Alpha-enolase	<0.01	3.9	109	47740/6.16
6	Dilhydrorimidinase-related protein 2	<0.05	6	125	62638/5.95
7	Glutamate synthetase	<0.05	6.4	91	42982/6.64
8	Glutamate dehydrogenase 1, mitochondrial precursor	<0.05	16.6	133	61640/8.05
9	Pyruvate kinase sozymes M1/M2	<0.05	5.9	227	58294/6.63
10	Fructose-bisphospate aldolase C	<0.01	10.3	109	39658/6.67
11	ATP synthase subunit alpha mitochondrial precursor	<0.04	9	232	59831/9.22

[†]For each protein, the carbonyl immunoreactivity/protein expression values were averaged ($n = 8$) and expressed as fold oxidation compared to control. The *p*-value listed is the significance of increased carbonyl levels relative to control aged samples (see text). pI = isoelectric point; Mr, relative mobility.

★Probability based MOWSE scores were estimated by comparison of search results against estimated random match population and were reported as $-10 \cdot \mathrm{LOG10}(p)$, where p is the absolute probability. A MOWSE score above 65 indicates a significant identity when searching in the total database.

TABLE III. Summary of the Proteins Identified by Redox Proteomics that Are Increasingly Carbonylated in the Cortex from Senescent Versus Aged Rats

Spot no.°	Protein name	Fold oxidation	*P* value	MOWSE score★	Mr/pI
1	Peroxiredoxin-2	10.1	0.05	91	21941/5.34
2	Guanine nucleotide-binding protein subunit beta-1	2 2	0.01	161	38151/5.60
3	Creatine kinase B-type	10.0	0.05	72	42052/5.39
4	Vacuolar ATP synthase subunit B, brain isoform	5.9	0.005	214	56857/5.95
5	Stress-70 protein, mitochondrial precursor	3.5	0.04	208	74094/5.37
6	Serine/threonine-protein phosphatase 2B catalytic subunit alpha isoform	4.1	0.04	86	59291/5.58
7	Aldehyde dehydrogenase, mitochondrial precursor	29.0	0.01	192	56966/6.63
8	Alpha-centractin	2.66	0.01	117	42701/6.19
9	Triosephosphate isomerase	4.8	0.01	161	27345/6.89
10	Glyceraldehyde-3-phosphate dehydrogenase	7.04	0.02	82	36090/8.97
11	Aspartate aminotransferase, cytoplasmic	3.4	0.01	239	46628/6.73
12	Pyruvate kinase isozymes M1/M2	2.8	0.04	175	58294/6.63
13	ATP synthase subunit alpha, mitochondrial precursor	5.1	0.04	205	59831/9.22
14	Fructose-bisphosphate aldolase A	4.7	0.04	188	39783/8.31
15	Glyceraldehyde-3-phosphate dehydrogenase	34.8	0.01	146	36090/8.14

TABLE IV. Summary of the Proteins Identified by Redox Proteomics That Are Increasingly Carbonylated in the Striatum From Senescent vs. Aged Rats

Spot no.	Protein name	*P* value	Fold oxidation	MOWSE score★	Mr/pI
1	Tubulin alpha-1A chain	<0.01	2.9	260	50788/4.94
2	78 kDa glucose-regulated protein	<0.05	3.8	146	72473/5.07
3	Stress-70 protein, mitochondria	<0.01	3.1	179	74097/5.37
4	Adenylate kinase isoenzyme	<0.05	3.0	94	21684/6.32
5	Elongation factor Tu, mitochondrial	<0.01	4.5	184	49890/7.23
6	Pyruvate kinase isozymes M1/M2	<0.05	10.6	71	49890/7.23
7	Pyruvate kinase isozymes M1/M2	<0.05	4.3	194	58294/6.63
8	Aconitate hydratase, mitochondrial	<0.05	3.3	240	86121/7.87
9	Triosephosphate isomerase	<0.05	4.0	97	27346/6.67
10	Glyceraldehyde-3-phosphate dehydrogenase	<0.05	9.9	151	36090/8.14

that no significant shift in the mitochondrial GSH redox state occurred, compared with that in the cytosol, among the two experimental group of animals.

Several studies from our laboratory and others have demonstrated that protein oxidation likely leads to protein dysfunction (Smith et al., 1991; Butterfield and Sultana, 2008; Suzuki et al., 2009). We measured the enzyme activity of some of the enzymes we found oxidized with the redox proteomics approach. Specifically, pyruvate kinase was found to be decreased in all the

TABLE V. Summary of the Proteins Identified by Redox Proteomics That Are Increasingly Carbonylated in the Cerebellum From Senescent vs. Aged Rats

Spot no.	Protein name	*P* value	Fold oxidation	MOWSE score*	Mr/pI
1	Heat shock cognate 71 kDa protein	<0.05	7.1	83	71244/5.37
2	Tubulin beta chain	<0.05	3.2	99	46994/4.78
3	Malate dehydrogenase, cytoplasmic	<0.05	2.8	75	36659/6.16
4	Isocitrate dehydrogenase [NAD] subunit alpha, mitochondria	<0.05	4.1	86	40044/5.94
5	Vesicle-fusing ATPase	<0.01	3.4	132	83170/6.55
6	Pyruvate kinase isozymes M1/M2	<0.05	4.4	114	58294/6.63
7	Synapsin-2	<0.05	2.8	75	63702/8.73
8	Aspartate aminotransferase, cytoplasmic	<0.01	5.2	131	46628/6.73
9	Phosphoglycerate kinase 1	<0.05	3.8	95	44909/8.02
10	Voltage-dependent anion-selective channel protein	<0.01	2.7	168	30851/8.62
11	Adenylate kinase isoenzyme 4, mitochondrial	<0.05	4.2	137	25301/7.79

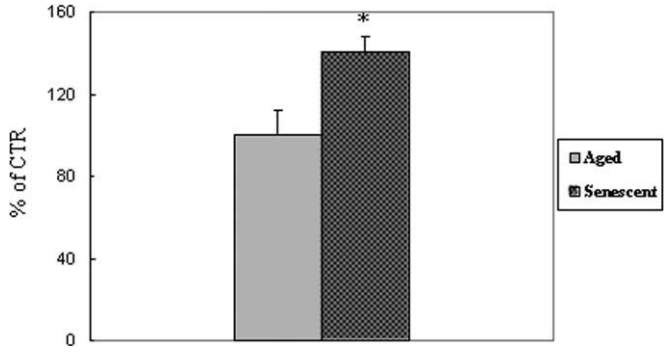

Fig. 3. Western blot analysis confirmed proteomic results of increased carbonyl levels of Hsp70 in senenscent rat hippocampus compared with aged rat using traditional immunochemical detection. Error bars indicate SEM for three samples in each group. *$P < 0.05$.

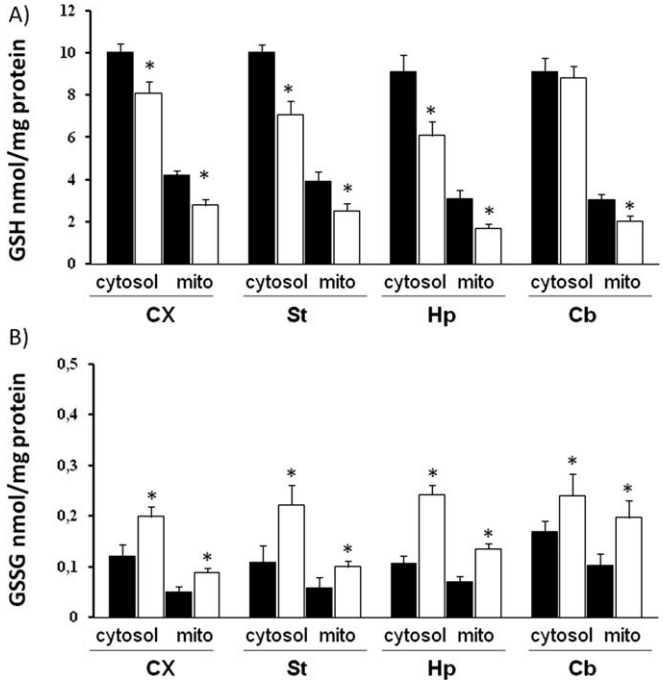

Fig. 4. Regional distribution of reduced glutathione (GSH) and oxidized glutathione (GSSG) in different brain regions in aged and senescent rats. Cytosolic (cytosol) and mitochondrial (mito) GSH (**A**) and GSSG (**B**) in cortex (CX), striatum (St), hippocampus (Hp), and cerebellum (Cb) were measured as described in Materials and Methods. Results are expressed in nmol/mg protein. Data are mean ± SEM of eight animals. *$P < 0.05$ vs. aged 12-month-old rats.

brain regions of senescent vs. aged rats (Fig. 5). In addition, the enzyme activity of GAPDH was found to be significantly decreased in both cortex and striatum of senescent rats compared with aged rats (Fig. 6). These results are in line with our previous findings of decreased enzyme activity of PK and GAPDH upon oxidation in AD brain in comparison with control brain (Sultana et al., 2009).

DISCUSSION

The free radical theory of aging of Harman (1956, 1992) proposes that oxidized macromolecules accumulate with age to decrease cell function and shorten life span. However, nutritional and genetic interventions to boost antioxidants have generally failed to increase life span (Gerschman et al., 1954; Gruber et al., 2008). The overall result of 19 clinical trials found that supplementation with the lipid-soluble antioxidant vitamin E failed to reduce mortality (Miller et al., 2005). The water-soluble antioxidant vitamin C is also generally ineffective in reducing all-cause mortality (Bjelakovic et al., 2007). An even more important test of the free radical theory of aging involves genetic overexpression of antioxidant enzymes. To date, increases in SOD, or catalase, or a combination, though lowering oxidized macromolecules, have failed to increase life span in mice (Perez et al., 2009). Only overexpression of the peroxide and redox-active thioredoxin 1 and mitochondria-targeted catalase (Brewer, 2009) have been shown to increase mouse life span. In their review of aging theories, Jang and Van Remmen (2009) conclude that these and other studies ''challenge'' the mitochondrial and free radical theories of aging, whereas Howes (2006) enumerates a list of failures of the free radical theory. A more complex regulation is suggested by experiments in *Caenorhabditis elegans*,

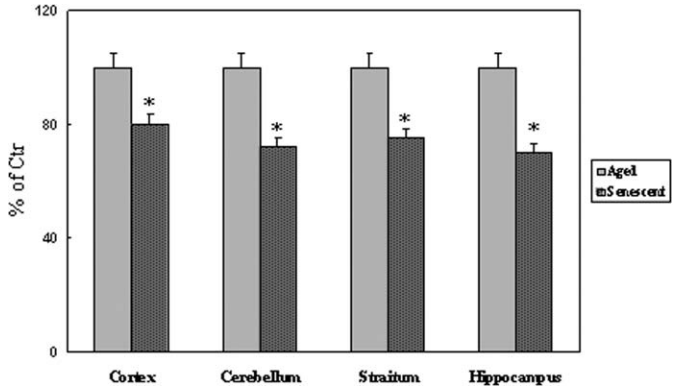

Fig. 5. Activity of PK in all the brain regions of senescent rats compared with aged controls. The activity of PK is significantly decreased in all the brain regions. Bars represent mean ± SE. $^*P < 0.05$; n = 8 for each group.

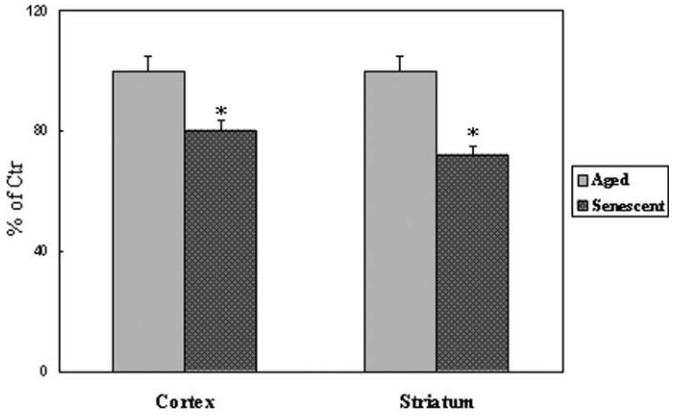

Fig. 6. Activity of GAPDH in cortex and striatum of senescent rats compared with aged control animals. $^*P < 0.05$.

in which careful titration with RNAi against mitochondrial function revealed a middle dose that promoted life span extension that was not correlated with oxidative stress (Brewer, 2009). In addition, the free radical theory fails to explain why higher levels of oxyradical damage occur with exercise (Brewer, 2009), which generally promotes healthy human aging (Mattson and Liu, 2002; Mattson, 2004) and extends life span in rats and in mice (Navarro et al., 2004).

GSH is the most prevalent nonprotein thiol in animal cells. De novo and salvage synthesis of GSH maintains a reduced cellular environment in which the tripeptide is a cofactor for cytoplasmic enzymes and can act as an important posttranslational modifier in a number of cellular proteins (Calabrese et al., 2002; Rebrin et al., 2007; Rebrin and Sohal, 2004, 2008). Because free radicals have defined roles in cell signalling events as well as in human disease pathologies (Calabrese et al., 2010a,b), an imbalance in expression of GSH and associated enzymes has been implicated in a variety of pathological conditions (Calabrese et al., 2009c). Thus, impaired function of the central nervous system (CNS) in aged animals is associated with increased susceptibility to the development of many neurodegenerative diseases, such as AD, PD, and ALS (Calabrese et al., 2007a, 2008, 2009b). In the present study, we show that oxidative stress increases during aging in brain, as revealed by decreased GSH content and increases in GSSG, particularly in the mitochondria, and this was associated with a specific pattern of protein oxidation at the inner mitochondrial membrane, where proteins of mitochondrial bioenergetics reside (Rebrin and Sohal, 2004).

Oxidatively damaged proteins are known to increase markedly with age (Cini and Moretti, 1995; Dogru-Abbasoglu et al., 1997; Butterfield and Sultana, 2008). In addition the loss of protein sulfhydryl groups and the reduced activity of important metabolic enzymes have been documented to occur in brain as a function of aging (Keller et al., 2000; Butterfield and Kanski, 2001; Zhu et al., 2006). Studies on the induction of the HSP response, a cytoprotective mechanism to counteract oxidative damage, showed a regional specificity indicating that different brain areas might undergo oxidation differently and react to protect themselves based on the strength of the insult (Calabrese et al., 2004, 2007b; Bellia et al., 2009).

Here we used a redox proteomics approach to identify the oxidatively modified proteins in four different brain regions of 28-month-old rats compared with 12-month-old rats. Interestingly, most of these proteins are involved in energy metabolism pathways, including ATP production, glycolysis, and the Krebs cycle. In addition, protein oxidation also affected components of the cell involved in cell structure, signal transduction, and the cellular stress response, such as Hsp70. The 70-kDa family of stress proteins includes the constitutive form of Hsp70, which includes Hsc70; the inducible form of Hsp70 (also referred to as Hsp72); and GRP78 (a constitutively expressed glucose-regulated protein found in the endoplasmic reticulum; Calabrese et al., 2006, 2008) and is a family of chaperone molecules contributing to cellular protection against a variety of stresses by preventing protein aggregation, assisting in the refolding of damaged proteins, and chaperoning nascent polypeptides along ribosomes. Hsp70 shows very low expression levels in brain under physiological conditions, but it is induced after certain oxidative stresses. Hsp70 is present in cytosol, nucleus, and endoplasmic reticulum (Calabrese et al., 2004). Inducible Hsp70 (Hsp72) has been found to have the highest levels in the substabtia nigra, followed by septum, cerebellum, striatum, hippocampus, and cortex (Calabrese et al., 2002, 2004, 2007b). Hsc70 is a constitutive isoform, recruited by the cell as a primary defense against unfavorable conditions. Previous studies in aged rats found that the basal level of Hsc70 was significantly higher in the substantia nigra, followed by septum and hippocampus, striatum, and cerebellum, with lowest levels in the cortex (Calabrese et al., 2002). Glucose-regulated protein 78 (GRP78) acts as a molecular chaperone by binding transiently to proteins crossing through the ER and helping their fold-

ing, assembly, and transport. GRP78 is the main constituent involved in the unfolded protein response. Decreased functionality of GRP78 can lead to a decreased activity of the proteasome, with consequently enhanced misfolded protein inside the cell (Hoozemans et al., 2005). Our findings on the oxidative modifications of these chaperone molecules in striatum, cerebellum, and cortex could lead to an increased accumulation of misfolded proteins, one of the main, common traits occurring in aging and neurodegenerative disorders (Perluigi et al., 2005; Pocernich et al., 2005; Poon et al., 2005a,b,c, 2006; Reed et al., 2008).

In the present study, we have identified several proteins that were significantly more oxidized in the brains of senescent vs. aged rats. The oxidatively modified proteins are in some cases similar to those found in AD brain (Castegna et al., 2002; Sultana et al., 2006a,b), thus confirming that aging is a major risk factor for developing neurodegenerative diseases. Although the etiologies are different and likely multifactorial, aging and age-related neurodegenerative diseases share some common pathological mechanisms, among which energy failure is one of the most crucial for neuronal dysfunction (Yap et al., 2009). In addition, the animal model of aging used in this study, which is based on naturally occurring phenotypes, may be particularly useful for the identification of biological markers and to provide new insight into the molecular mechanism of brain development, aging, and neurodegeneration.

REFERENCES

Ashok BT, Ali R. 1999. The aging paradox: free radical theory of aging. Exp Gerontol 34:293–303.

Beckman KB, Ames BN. 1998. The free radical theory of aging matures. Physiol Rev 78:547–581.

Boveris A, Navarro A. 2008. Brain mitochondrial dysfunction in aging. IUBMB Life 60:308–314.

Bellia F, Calabrese V, Guarino F, Cavallaro M, Cornelius C, De Pinto V, Rizzarelli E. 2009. Carnosinase levels in aging brain: redox state induction and cellular stress response. Antiox Redox Signal 11:2759–2775.

Bjelakovic G, Nikolova D, Gluud LL, Simonetti RG, Gluud C. 2007. Mortality in randomized trials of antioxidant supplements for primary and secondary prevention: systematic review and meta-analysis. JAMA 297:842–857.

Brewer GJ. 2009. Epigenetic oxidative redox shift (EORS) theory of aging unifies the free radical and insulin signaling theories. Exp Gerontol (in press).

Butterfield DA, Kanski J. 2001. Brain protein oxidation in age-related neurodegenerative disorders that are associated with aggregated proteins. Mech Ageing Dev 122:945–962.

Butterfield DA, Sultana R. 2008. Redox proteomics: understanding oxidative stress in the progression of age-related neurodegenerative disorders. Expert Rev Proteom 5:157–160.

Butterfield DA, Koppal T, Howard B, Subramaniam R, Hall N, Hensley K, Yatin S, Allen K, Aksenov M, Aksenova M, Carney J. 1998. Structural and functional changes in proteins induced by free radical-mediated oxidative stress and protective action of the antioxidants N-tert-butyl-alpha-phenylnitrone and vitamin E. Ann N Y Acad Sci 854:448–462.

Calabrese V. 2007. Highlight commentary on "Redox proteomics analysis of oxidatively 3 modified proteins in G93A-SOD1 transgenic mice—a model of 4 familial amyotrophic lateral sclerosis." Free Radic Biol Med 43:160–162.

Calabrese V, Scapagnini G, Giuffrida Stella AM, Bates TE, Clark JB. 2001. Mitochondrial involvement in brain function and dysfunction: relevance to aging, neurodegenerative disorders and longevity. Neurochem Res 26:739–764.

Calabrese V, Scapagnini G, Ravagna A, Fariello RG, Giuffrida Stella AM, Abraham NG. 2002. Regional distribution of heme oxygenase, HSP70, and glutathione in brain: relevance for endogenous oxidant/antioxidant balance and stress tolerance. J Neurosci Res 68:65–75.

Calabrese V, Scapagnini G, Ravagna A, Colombrita C, Spadaro F, Butterfield DA, Giuffrida Stella AM. 2004. Increased expression of heat shock proteins in rat brain during aging: relationship with mitochondrial function and glutathione redox state. Mech Ageing Dev 125:325–335.

Calabrese V, Butterfield DA, Scapagnini G, Stella AM, Maines MD. 2006. Redox regulation of heat shock protein expression by signaling involving nitric oxide and carbon monoxide: relevance to brain aging, neurodegenerative disorders, and longevity. Antiox Redox Signal 8:444–477.

Calabrese V, Mancuso C, Calvani M, Rizzarelli E, Butterfield DA, Giuffrida Stella AM. 2007a. Nitric oxide in the CNS: neuroprotection versus neurotoxicity. Nat Neurosci 8:766–775.

Calabrese V, Mancuso C, Ravagna A, Perluigi M, Cini C, De Marco C, Butterfield DA, Giuffrida Stella AM. 2007b. In vivo induction of heat shock proteins in the substantia nigra following L-DOPA administration is associated with increased activity of mitochondrial complex I and nitrosative stress in rats: regulation by glutathione redox state. J Neurochem 101:709–717.

Calabrese V, Cornelius C, Mancuso C, Pennisi G, Calafato S, Bellia F, Bates TE, Giuffrida Stella AM, Schapira T, Dinkova Kostova AT, Rizzarelli E. 2008. Cellular stress response: a novel target for chemoprevention and nutritional neuroprotection in aging, neurodegenerative disorders and longevity. Neurochem Res 33:2444–2471.

Calabrese V, Cornelius C, Dinkova-Kostova AT, Calabrese EJ. 2009a. Vitagenes, cellular stress response and acetylcarnitine: relevance to hormesis. Biofactors 35:146–160.

Calabrese V, Cornelius C, Mancuso C, Barone E, Calafato S, Bates T, Rizzarelli E, Kostova AT. 2009b. Vitagenes, dietary antioxidants and neuroprotection in neurodegenerative diseases. Front Biosci 14:376–397.

Calabrese V, Cornelius C, Rizzarelli E, Owen JB, Dinkova-Kostova AT, Butterfield DA. 2009c. Nitric oxide in cell survival: a Janus molecule. Antiox Redox Signal 11:2717–2739.

Calabrese V, Cornelius C, Trovato A, Cavallaro M, Di Rienzo L, Condorelli D, De Lorenzo A, Calabrese EJ. 2010a. The hormetic role of dietary antioxidants in free radical-related diseases. Curr Pharm Des (in press).

Calabrese V, Cornelius C, Mancuso C, Lentile R, Stella AM, Butterfield DA. 2010b. Redox homeostasis and cellular stress response in aging and neurodegeneration. Methods Mol Biol 610:285–308.

Carney JM, Starke-Reed PE, Oliver CN, Landum RW, Cheng MS, Wu JF, Floyd RA. 1991. Reversal of age-related increase in brain protein oxidation, decrease in enzyme activity, and loss in temporal and spatial memory by chronic administration of the spin-trapping compound N-tert-butyl-alpha-phenylnitrone. Proc Natl Acad Sci U S A 88:3633–3636.

Castegna A, Aksenov M, Aksenova M, Thongboonkerd V, Klein JB, Pierce WM, Booze R, Markesbery WR, Butterfield DA. 2002. Proteomic identification of oxidatively modified proteins in Alzheimer's disease brain. Part I: creatine kinase BB, glutamine synthase, and ubiquitin carboxy-terminal hydrolase L-1. Free Radic Biol Med 33:562–571.

Cini M, Moretti A. 1995. Studies on lipid peroxidation and protein oxidation in the aging brain. Neurobiol Aging 16:53–57.

Dogru-Abbasoglu S, Tamer-Toptani S, Ugurnal B, Kocak-Toker N, Aykac-Toker G, Uysal M. 1997. Lipid peroxidation and antioxidant enzymes in livers and brains of aged rats. Mech Ageing Dev 98:177–180.

Gerschman R, Gilbert DL, Nye SW, Dwyer P, Fenn WO. 1954. Oxygen poisoning and x-irradiation: a mechanism in common. Science 119:623–626.

Gruber J, Schaffer S, Halliwell B. 2008. The mitochondrial free radical theory of ageing—where do we stand? Front Biosci 13:6554–6579.

Harman D. 1956. Aging: a theory based on free radical and radiation chemistry. J Gerontol 11:298–300.

Harman D. 1992. Free radical theory of aging. Mutat Res 275:257–266.

Hoozemans JJ, Veerhuis R, Van Haastert ES, Rozemuller JM, Baas F, Eikelenboom P, Scheper W. 2005. The unfolded protein response is activated in Alzheimer's disease. Acta Neuropathol 110:165–172.

Howes RM. 2006. The free radical fantasy: a panoply of paradoxes. Ann N Y Acad Sci 1067:22–26.

Jang YC, Van Remmen H. 2009. The mitochondrial theory of aging: insight from transgenic and knockout mouse models. Exp Gerontol 44:256–260.

Keller JN, Hanni KB, Markesbery WR. 2000. Possible involvement of proteasome inhibition in aging: implications for oxidative stress. Mech Ageing Dev 113:61–70.

Lenaz G, Bovina C, D'Aurelio M, Fato R, Formiggini G, Genova ML, Giuliano G, Merlo Pich M, Paolucci U, Parenti Castelli G, Ventura B. 2002. Role of mitochondria in oxidative stress and aging. Ann N Y Acad Sci 959:199–213.

Mattson MP. 2004. Pathways towards and away from Alzheimer's disease. Nature 430:631–639.

Mattson MP, Liu D. 2002. Energetics and oxidative stress in synaptic plasticity and neurodegenerative disorders. Neuromol Med 2:215–231.

Miller ER, 3rd, Pastor-Barriuso R, Dalal D, Riemersma RA, Appel LJ, Guallar E. 2005. Meta-analysis: high-dosage vitamin E supplementation may increase all-cause mortality. Ann Intern Med 142:37–46.

Navarro A, Gomez C, Lopez-Cepero JM, Boveris A. 2004. Beneficial effects of moderate exercise on mice aging: survival, behavior, oxidative stress, and 605 mitochondrial electron transfer. Am J Physiol Regul Integr Comp Physiol 286:R505–R511.

Perez VI, Van RH, Bokov A, Epstein CJ, Vijg J, Richardson A. 2009. The overexpression of major antioxidant enzymes does not extend the lifespan of 630 mice. Aging Cell 8:73–75.

Perluigi M, Poon HF, Maragos W, Pierce WM, Klein JB, Calabrese V, Cini C, De Marco C, Butterfield DA. 2005. Proteomic analysis of protein expression and oxidative modification in r6/2 transgenic mice: a model of Huntington disease. Mol Cell Proteom 4:1849–1861.

Pocernich CB, Poon HF, Boyd-Kimball D, Lynn BC, Nath A, Klein JB, Butterfield DA. 2005. Proteomic analysis of oxidatively modified proteins induced by the mitochondrial toxin 3-nitropropionic acid in human astrocytes expressing the HIV protein tat. Brain Res Mol Brain Res 133:299–306.

Poon HF, Frasier M, Shreve N, Calabrese V, Wolozin B, Butterfield DA. 2005a. Mitochondrial associated metabolic proteins are selectively oxidized in A30P alpha-synuclein transgenic mice—a model of familial Parkinson's disease. Neurobiol Dis 18:492–498.

Poon HF, Hensley K, Thongboonkerd V, Merchant ML, Lynn BC, Pierce WM, Klein JB, Calabrese V, Butterfield DA. 2005b. Redox proteomics analysis of oxidatively modified proteins in G93A-SOD1 transgenic mice—a model of familial amyotrophic lateral sclerosis. Free Radic Biol Med 39:453–462.

Poon HF, Vaishnav RA, Butterfield DA, Getchell ML, Getchell TV. 2005c. Proteomic identification of differentially expressed proteins in the aging murine olfactory system and transcriptional analysis of the associated genes. J Neurochem 94:380–392.

Poon HF, Shepherd HM, Reed TT, Calabrese V, Stella AM, Pennisi G, Cai J, Pierce WM, Klein JB, Butterfield DA. 2006. Proteomics analysis provides insight into caloric restriction mediated oxidation and expression of brain proteins associated with age-related impaired cellular processes: mitochondrial dysfunction, glutamate dysregulation and impaired protein synthesis. Neurobiol Aging 27:1020–1034.

Rebrin I, Sohal RS. 2004. Comparison of thiol redox state of mitochondria and homogenates of various tissues between two strains of mice with different longevities. Exp Gerontol 39:1513–1519.

Rebrin I, Sohal RS. 2008. Pro-oxidant shift in glutathione redox state during aging. Adv Drug Deliv Rev 60:1545–1552.

Rebrin I, Forster MJ, Sohal RS. 2007. Effects of age and caloric intake on glutathione redox state in different brain regions of C57BL/6 and DBA/2 mice. Brain Res 1127:10–18.

Reed T, Perluigi M, Sultana R, Pierce WM, Klein JB, Turner DM, Coccia R, Markesbery WR, Butterfield DA. 2008. Redox proteomic identification of 4-hydroxy-2-nonenal-modified brain proteins in amnestic mild cognitive impairment: insight into the role of lipid peroxidation in the progression and pathogenesis of Alzheimer's disease. Neurobiol Dis 30:107–120.

Smith CD, Carney JM, Starke-Reed PE, Oliver CN, Stadtman ER, Floyd RA, Markesbery WR. 1991. Excess brain protein oxidation and enzyme dysfunction in normal aging and in Alzheimer disease. Proc Natl Acad Sci U S A 88:10540–10543.

Stadtman ER. 1988. Biochemical markers of aging. Exp Gerontol 23:327–347.

Stadtman ER, Berlett BS. 1998. Reactive oxygen-mediated protein oxidation in aging and disease. Drug Metab Rev 30:225–243.

Sultana R, Newman SF, Abdul HM, Cai J, Pierce WM, Klein JB, Merchant M, Butterfield DA. 2006a. Protective effect of D609 against amyloid-beta1–42-induced oxidative modification of neuronal proteins: redox proteomics study. J Neurosci Res 84:409–417.

Sultana R, Poon HF, Cai J, Pierce WM, Merchant M, Klein JB, Markesbery WR, Butterfield DA. 2006b. Identification of nitrated proteins in Alzheimer's disease brain using a redox proteomics approach. Neurobiol Dis 22:76–87.

Sultana R, Perluigi M, Butterfield DA. 2009. Oxidatively modified proteins in Alzheimer's disease (AD), mild cognitive impairment and animal models of AD: role of Abeta in pathogenesis. Acta Neuropathol 118:131–150.

Suzuki YJ, Carini M, Butterfield DA. 2009. Protein carbonylation. Antiox Redox Signal (in press).

Van Remmen H, Richardson A. 2001. Oxidative damage to mitochondria and aging. Exp Gerontol 36:957–968.

Yap LP, Garcia JV, Han D, Cadenas E. 2009. The energy-redox axis in aging and age-related neurodegeneration. Adv Drug Deliv Rev (in press).

Zhu Y, Carvey PM, Ling Z. 2006. Age-related changes in glutathione and glutathione-related enzymes in rat brain. Brain Res 1090:35–44.